Available online on 15.09.2024 at http://jddtonline.info

Journal of Drug Delivery and Therapeutics

Open Access to Pharmaceutical and Medical Research

Open Access Full Text Article

Research Article

Virtual design and screening of new (+)-catechin derivates N- and/or *S-heterocyclic* fragment for anti-malarial and anti-*SARS-CoV-2* activities by In silico simulation

Ahmed Said Mohamed [1]*, Imane Yamari [2], Nouh Mounadi [2], Abdirahman Elmi [1], Mohammed Bouachrine [3], Hanane Zaki [3], Samir Chtita [2]

[1] *Centre d'Étude et de Recherche de Djibouti, Institut de Recherche Médicinale, Route de l'aéroport, Djibouti.*
[2] *Laboratory Physical Chemistry of Materials, Faculty of Sciences Ben M'Sik, Hassan II University of Casablanca, B.P. 7955 Sidi Othmane, Casablanca, Morocco.*
[3] *Bio Laboratory, Higher School of Technology Khenifra, Sultane Moulay Slimane University, Khenifra, Morocco.*

Article Info:

Article History:

Received 24 June 2024
Reviewed 03 August 2024
Accepted 25 August 2024
Published 15 Sep 2024

Cite this article as:

Mohamed AS, Yamari I, Mounadi N, Elmi A, Bouachrine M, Zaki H, Chtita S, Virtual design and screening of new (+)-catechin derivates *N*- and/or *S-heterocyclic* fragment for anti-malarial and anti-*SARS-CoV-2* activities by *In silico* simulation, Journal of Drug Delivery and Therapeutics. 2024; 14(9):35-50

DOI: http://dx.doi.org/10.22270/jddt.v14i9.6762

*Address for Correspondence:

Ahmed Said Mohamed, Centre d'Étude et de Recherche de Djibouti, Institut de Recherche Médicinale, Route de l'aéroport, Djibouti.

Abstract

Hemisynthesis makes it possible to improve the activity or reduce the toxicity of a biocompound by modifying or adding peripheral groups. Catechin present in different plant species was known for its moderate anti-malarial and anti-*SARS-CoV-2* activities. The aim of this work was focused on the identification of new compounds with potential anti-*SARS-CoV-2* and/or anti-malarial activities, evaluated through *In silico* simulation. A polyphenol pharmacophore model, based on (+)-catechin (**1**) was virtually constructed using previously reported inhibitors. *N*- and/or *S*-heterocyclic fragments were inserted on the backbone of (+)-catechin and 12 pharmacophore hypotheses were studied. This study targeted 3 proteins biologically responsible for SARS-CoV-2 (PDB ID: *7JYC*, *6M0J*, and *6HZD*) and one protein responsible for malaria (PDB ID: *3SRJ*). Molecular docking had shown that the new catechin-aldehyde candidates have good Ligand-Protein affinity in terms of free energy compared to the study reference Narlaprevir and Artesunate for *SARS-CoV-2* and malaria respectively. Theoretically, most compounds didn't show toxicity except compounds **2a**, **2i,** and **2k**, exhibiting hepatotoxic activity. Molecular dynamics was used to prove and assess their binding stability to the target protein for each activity. The *3SRJ*-**2f** and *6HZD*-**2l** structures were selected for anti-malarial and anti-*SARS-CoV-2* activity respectively. The *3SRJ*-**2f** and *6HZD*-**2l** complexes showed stable interactions to 100 ns between the inhibitor fragments and the residual amino acids of the protein. To conclude, these novel compounds are probably to become promising lead molecules for the development of effective anti-*SARS-CoV-2* and/or anti-malarial of all drugs.

Keywords: Catechin, Anti-malarial, Anti-SARS-CoV-2, Docking and Dynamic Molecular, ADMET Analysis.

1. INTRODUCTION

Catechin is a natural compound of the flavonoid family, often found in green tea but also in some medicinal plants such as the fruits of the *Acacia catechu* [1] or also in bark of *Acacia seyal* of Republic of Djibouti [2]. It was characterized by its colorless shade, its good solubility in water and by its molecular structure, bearing two phenolic rings separated by a central heterocyclic and its several hydroxyl groups. Catechin well known for their potential antioxidant properties [3–5]. Several studies have been carried out, showing the beneficial effect of catechin for the prevention of certain types of cancers [6–8], reduction of the risks of obesity, diabetes, and cardiovascular diseases and improvement of the immune system. It was also shown that catechin or catechin derivates can be a promising candidate for anti-malarial [9–13] and anti-*SARS-CoV-2* activities[14–16].

A. R. Sannella *et al.,* in 2007 showed by *in vitro* anti-malarial test that the two main constituents: epigallocatechin-3-gallate (EGCG) and epicatechin gallate (ECG) of catechin derivatives and crude extract of green tea inhibit the growth of *Plasmodium falciparum*. In addition, epigallocatechin-3-gallate (EGCG) and epicatechin gallate (ECG) have also been shown to potentiate, at least moderately, the antiplasmodial effects of artemisinin, when the latter is administered at sublethal doses [17].

A study was also carried out by Iwan Budiman *et al.,* in 2015, to evaluate anti-malarial activities of various catechins including catechin (C), epicatechin (EC), catechin-gallate (CG), gallocatechingallate (GCG), epigallocatechin (EGC), epicatechin-gallate (ECG), epigallocatechin-gallate (EGCG). The IC_{50} of catechins in *Plasmodium falciparum* after 48 hours incubation compared to a reference Artemisinin. This work showed that the most active anti-malarial activity was CG (IC_{50}= 0.366 µM) and the lowest anti-malarial activity was EGC (IC_{50} = 98.145 µM). C, EC, CG grouped as active anti-malarial activity with IC_{50}: 0.734, 0.456, and 0.366 µM respectively; GC (7.457 µM), ECG (2.049 µM), EGCG (5.633 µM) as moderate active anti-malarial activity; GCG, and EGC as very weak anti-malarial activity [18]. These studies confirm that structural modification plays a key role in the influence of anti-malarial activity.

Graphical abstract

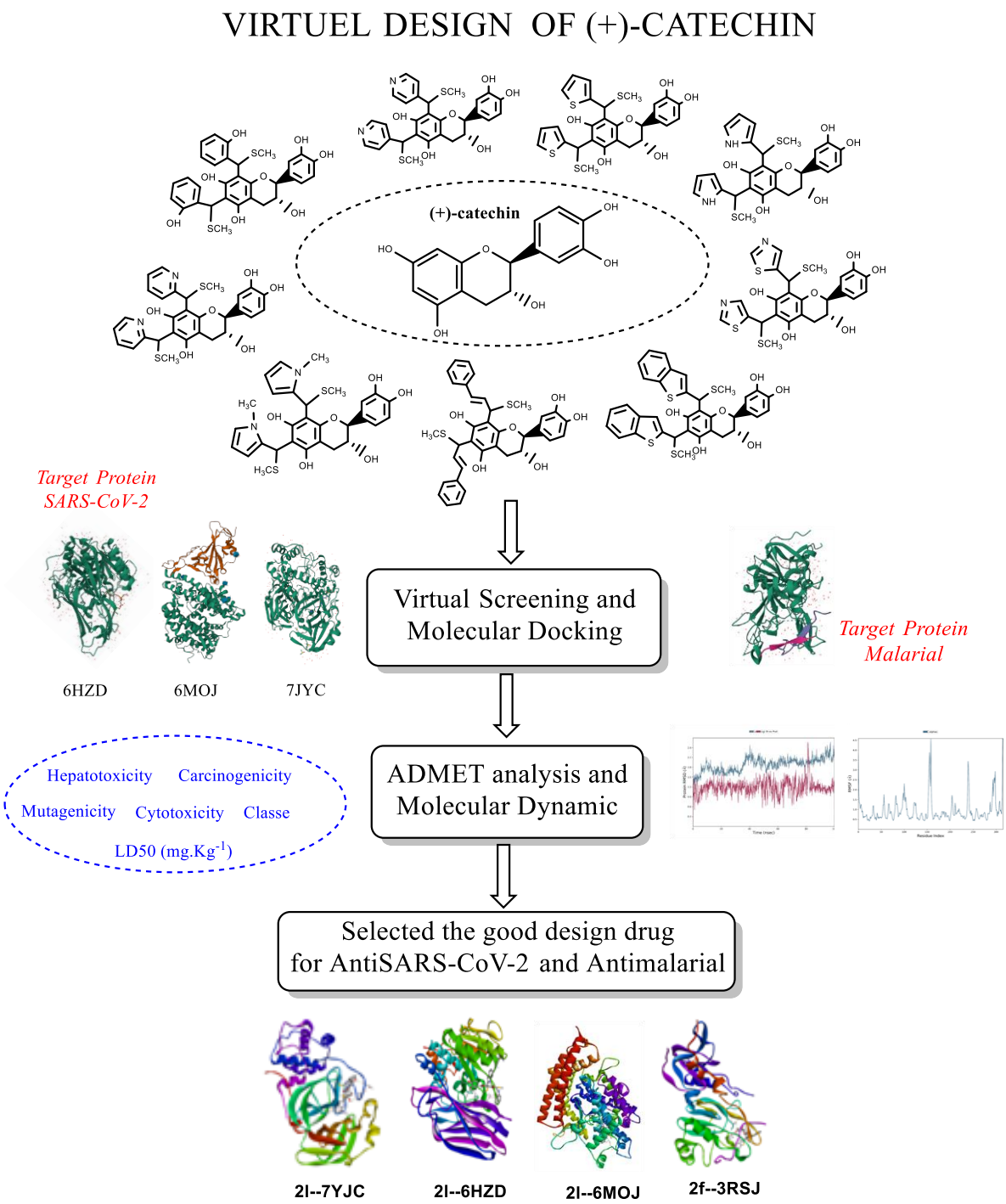

The appearance of Covid-19 at the end of 2019, researchers are also focused on finding attempts to stop this global pandemic[19]. In 2020 to 2023, several studies were published evaluating certain natural substances by *In silico* and/or by *In vitro* as anti-Covid-19 agents [20–23]. Catechin and its derivatives are also being tested against SARS-CoV-2 [24–26].

The *in silico* studies carried out by Susmit Mhatre *et al.*, in 2021 showed that the catechins and its derivates form favorable interactions with the spike protein (The prefusion *SARS-CoV-2* spike glycoprotein (wild and mutated strains): PDB ID: *6VSB*) and can potentially impair its function. Epigallocatechin gallate (EGCG) showed the best binding (-6.3, and -6.4 kJ/mol wild and mutated strains respectively) among the catechin against both the strains. The results are encouraging for further exploration of the antiviral activity of EGCG against *SARS-CoV-2* and its variants[27].

A recent study by Shaik *et al.,* in 2022 highlights the role of catechins as entry-inhibitors against *SARS-CoV-2* by *in silico*. The lead compounds were EGCG and ECG act as potential inhibitors bind to the active site region of the HKU4eCoV 3C-like protease (PDB ID: *4YOG)* and M-Pro protease (PDB ID: *7CAM*) enzymes of coronavirus[28].

The objective of this work was to evaluate catechin and its derivatives against two biological activities namely anti-*SARS-CoV-2* and *anti-plasmodium* activities through *in silico* simulation. Hypothetically, the idea is to decorate the (+)-catechin skeleton with heterocyclic fragments (*N*- and/or *S*-) to study the relationship between biological activity and the different catechin structures. This work was carried out by choosing 3 proteins responsible for the *SARS-CoV-2* virus (*SARS-CoV-2* main protease (3CLpro/Mpro) in complex with covalent inhibitor Narlaprevir, PDB ID: *7JYC*[29,30]; X-ray structure of furin in complex with the cyclic inhibitor

c[glutaryl-Arg-Arg-Arg-Lys]-Arg-4-Amba, PDB ID: *6HZD*[31,30]; and crystal structure of *SARS-CoV-2* spike receptor-binding domain bound with ACE2, PDB ID: *6MOJ* [32,30] and a protein responsible for the *Plasmodium falciparum* parasite; PDB ID: *3SRJ* (PfAMA1 in complex with invasion-inhibitory peptide R1)[33,30]. Subsequently, an ADMET study is also done to predict the toxicity of these future compounds. The best compound of each activity (Anti-SARS-CoV-2 and *anti-plasmodium* activities) was studied by molecular dynamics to see the stability of the compound-protein interaction.

2. MATERIALS AND METHODS

*2.1 Proposal of (+)-catechin derivative structures (**2**).*

The serie of catechin derivatives were inspired by the work carried out by Katsuko Kajiya *et al.,* in 2004. Generally, the type of compound was obtained by reaction of aldehyde and (+)-catechin in acid medium in the presence of methyl mercaptan[34].

Compounds **2a-l** were virtually designed with existing aldehyde at Sigma Aldrich, to assess their biological capacity for anti-malarial and anti-*SARS-CoV-2* activities through bioinformatics. The skeleton of (+)-catechin was modified on the two carbon positions C6 and C8 of ring A with homo-heterocyclic fragments. For that, the *3D*-structures of the 12 inhibitors were prepared using a molecule editor in ChemDraw professional 15.0 and were generated for all ligands with LigPrep.

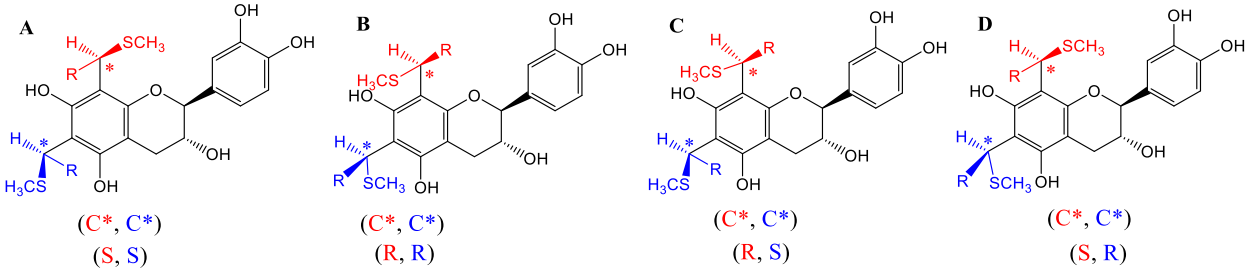

Chart 1: Different stereoisomer of compound (+)-catechin-aldehyde.

Generally, the experimental reaction resulted in a mixture of four stereoisomers, due to the presence of two other asymmetric carbons carried by the carbon position 6 and 8 (Chart 1). In the context of this article, the simulation was carried out with an identical structural conformation, giving the (*R, R*) stereoisomer for all the structures except for compounds **2a**, and **2b** with an (*S, S*) configuration (Table 1).

Table 1: Details of virtual screening compounds.

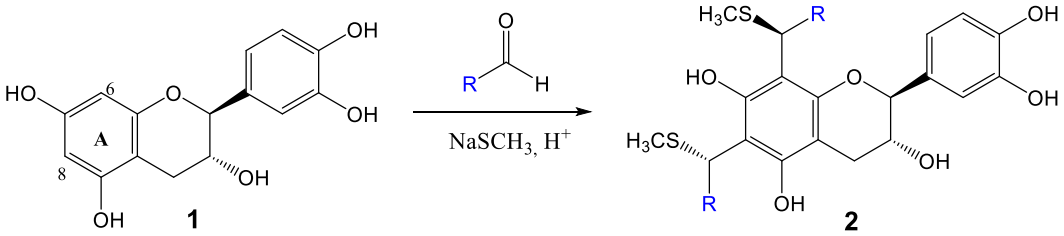

Ligands	Aldéhyde names	Structures
2a	2-hydroxycarboxaldehyde	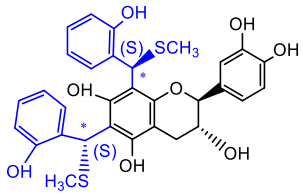
2b	4-Pyridinecarboxaldehyde	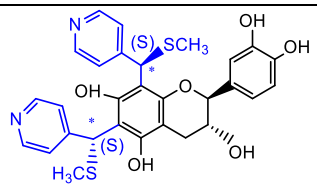
2c	2-Thiophenecarboxaldehyde	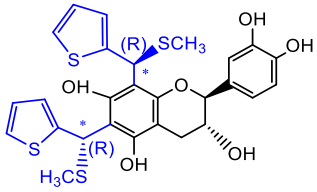

2d	Pyrrole-2-carboxaldehyde	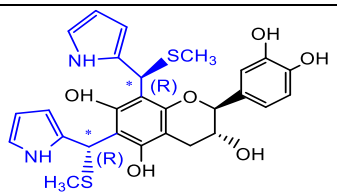
2e	Cinnamaldehyde	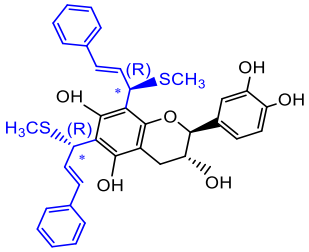
2f	Benzo[b]thiophene-2-carboxaldehyde	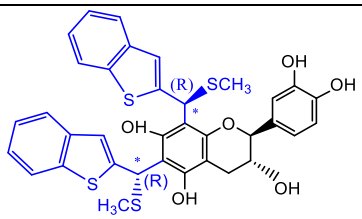
2g	2-Pyridinecarboxaldehyde	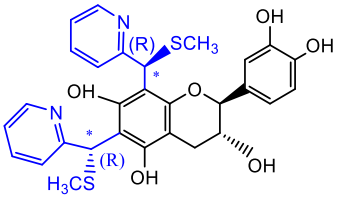
2h	*N*-Methyl-2-pyrrolecarboxaldehyde	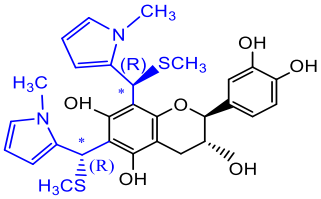
2i	5-Thiazolecarboxaldehyde	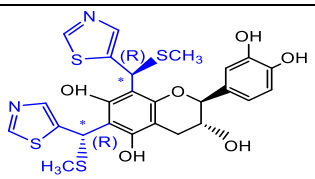
2j	5-Oxazolecarboxaldehyde	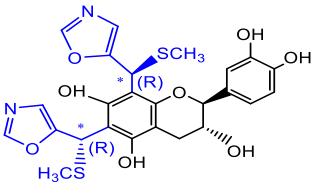
2k	Benzothiazole-2-carboxaldehyde	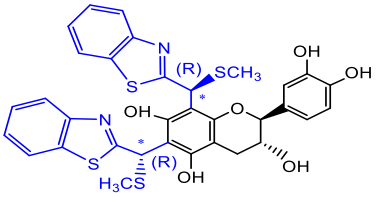
2l	Indole-3-carboxaldehyde	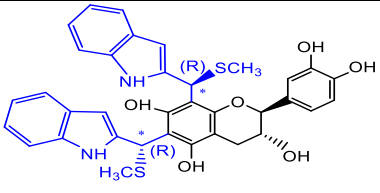

2.2. In silico study of (+)-catechin derivate compounds.

2.2.1. Molecular Docking.

Molecular docking studies were performed using Autodock Vina software[35,36] to evaluate the affinity of 12 (+)-catechin derivates toward *SARS-CoV-2* and *Plasmodium falciparum* activities. 12 ligands and the control drug Narlaprevir for anti-*SARS-CoV-2* activity were docked into the receptor pocket of (3CLpro/Mpro) in complex with covalent Inhibitor Narlaprevir (PDB code: *7YJC*) also with furin in complex with the cyclic inhibitor c[glutaryl-Arg-Arg-Arg-Lys]-Arg-4-Amba (PDB code: *6HZD*) and the spike receptor-binding domain bound with ACE2 (PDB ID: *6M0J*). The *Anti-plasmodium* activity for 12 ligands and the control drug Artesunate [37] were docked into the receptor pocket of PfAMA1 in complex with invasion-inhibitory peptide R1 (PDB ID: *3SRJ*). The crystal structures of protein targets for anti-*SARS-CoV-2* and Anti-plasmodium falciparum compounds were downloaded from the RCSB Protein Data Bank available online at (www.RCSB.org/structure). Before performing docking, all ligand linked to the crystal structure of protein targets were removed and then Kollman charges as well as polar hydrogen were added using AutoDockTools[38]. The docking gird box was set as follow: x =50, y = -34.77, z = -6 for furin in complex with the cyclic inhibitor c[glutaryl-Arg-Arg-Arg-Lys]-Arg-4-Amba (PDB ID: *6HZD*), x = -22.928, y = 12.346, z = -1.572 for the spike receptor-binding domain bound with ACE2 (PDB ID: *6M0J*), x = 123.488, y =2.092, z = 22.240 for the receptor pocket of (3CLpro/Mpro) in complex with Covalent Inhibitor Narlaprevir (PDB ID: *7JYC*), and x = 17.076, y = 11.499, z = 42.949 for PfAMA1 in complex with invasion-inhibitory peptide R1 (PDB ID: *3SRJ*) at 40 Å size and 0.375 Å spacing. Furthermore, the ligand structures were optimized with the steepest Descent method using Avogadro software[39] and then Gasteiger charges were added to the optimized structures, followed by merging no polar hydrogens. Finally, the investigated ligands were docked to the target protein and the involved interactions were analyzed employing Discovery Studio 2021 software[40].

2.2.2 Analyzing ADMET.

ADMET (Absorption, Distribution, Metabolism, Elimination, Toxicity) analysis were calculated using the Swiss adme[41] for assessing the drug ability and to filter the ligand molecules at an early stage of identifying the new inhibitors. Toxicity was the degree to which a substance can damage an organism or substructure of the organism. The predictions of toxicity of the compounds were essential to reduce the cost and labor of a drug's preclinical and clinical trials. The toxicity evaluation was performed also using the ProTox platform [42]. It gave predicted toxicity values, cytotoxicity, mutagenicity, carcinogenicity, immunotoxicity, and LD50 values of selected compounds.

2.2.3 Dynamic Molecular Simulation.

We were interested to two structures showing highest binding affinity, one towards anti-*plasmodium* (*3SRJ*–**2f**) and another for anti-*SARS-CoV-2* (*6HZD*–**2l**) were selected for Molecular Dynamics Simulation (MDS) studies. Using the OPLSe3 force field[43], the MDS was conducted with Schrodinger Desmond software[44] to analyze the movements of biomolecule atoms in the presence of tiny molecules and to determine the stability of ligand-protein interactions[45–47]. A basic point charge water model SPC was used in the simulation. To balance the MD-simulated net charge system, the protein-ligand complex was neutralized by adding Na^+ or Cl^- ions, and 0.15 M NaCl was maintained to replicate a physiological ion concentration. The simulation was then run in an orthorhombic box with a 10 Å x 10 Å x 10 Å dimensional space and NPT ensemble, starting with 1 ns at NVT equilibrium at 300 K, followed by 100 ns at standard pressure (1.01325 bar)[48]. Root Mean Square Deviation (RMSD), Root Mean Square Fluctuation (RMSF), and protein-ligand interaction were among the metrics measured by MDS.

3. RESULTS AND DISCUSSIONS

3.1. Anti-SARS-CoV-2 *activity.*

3.1.1. Bibliographic study of catechin and its derivatives against SARS-CoV-2 by in silico.

Table 2: Study comparisons carried out by *in silico* for catechin and its derivatives against SARS-CoV-2.

Name of compound	Binding Energy Kcal/mol	PDB ID	Targed Protein	References
Epicatechin-gallate	-7.52	*4YOG*	Catalytic Residues of 3C-like protease	28
Epigallocatechin-3-gallate	-7.25			
Epicatechin-gallate	-6.85	*7CAM*	Catalytic Residues of M-Pro protease	
Epigallocatechin-3-gallate	-7.57			
Epigallocatechin	-7.0	*6LU7*	The SARS CoV-2 Mpro	49
Gallocatechin	-7.1			
Catechin	-7.1			
Epicatechin	-7.2			
Catechin-gallate	-7.2			
Epigallocatechin-3-gallate	-7.6			
Epicatechin-gallate	-8.2			
Gallocatechingallate	-9.0			
Epigallocatechin-3-gallate	-7,8	*6M17*	The spike receptor-binding domain (RBD) and human cell receptor angiotensin-converting	50

			enzyme 2 (ACE2)	
Epigallocatechin-3-gallate	-8,601	*7CMD*	*SARS-CoV-2* PLProprotein	51
Epicatechin-gallate	-8,566			
Gallocatechingallate	-7,865			
Catechin-gallate	-7,498			
Gallocatechin	-6,337			
(-)-Catechin	-6,329			
Epigallocatechin	-6,318			
Epicatechin	-6,128			
(-)-Catechin	-14.1370	*6LU7*	Receptor main Protease	52
(+)-Catechin	-13.5387			
(-)-Epicatechin	-13.6338			
(+)-Epicatechin	-12.2790			
(-)-Catechin gallate	-12.9942			
(+)-Catechin gallate	-13.7186			
Catechin 3'-O-gallate	-14.4852			
Catechin 5-O-gallate	-14.6331			
Catechin 7-O-gallate	-15.0299			
Catechin 3'-glucoside	-12.3104			
Catechin 5-glucoside	-11.9737			
(-)-Catechin	-11.3222	*6LXT*	Receptor spike glycoprotein	
(+)-Catechin	-10.4993			
(-)-Epicatechin	-11.5055			
(+)-Epicatechin	-10.3292			
(-)-Catechin gallate	-12.4199			
(+)-Catechin gallate	-13.0183			
Catechin 3'-O-gallate	-11.8377			
Catechin 5-O-gallate	-11.3650			
Catechin 7-O-gallate	-11.9637			
Catechin 3'-glucoside	-10.5722			
Catechin 5-glucoside	-10.8447			
(+)-Catechin	-4.89	*6MOJ*	ACE2	53
	-8.34	*6M2N*	3-chymotrypsin-like cysteine protease (3CLpro)	
	-7.68	*6F06*	CTSL	
	-6.23	*6M3M*	Crystal structure of nucleocapsid protein	
	ND	*6M71*	RdRp	
	-7.04	*NSP6*	non-structural protein 6	
	-5.79	*7BV2*	cryo–electron microscopy structure of RdRp enzyme remdesivir and NSP12-NSP7-NSP8 complex	
	-7.240	*6LUZ*	3CLpro/Mpro	54
	-7.677	*5R84*	*SARS-CoV-2* Mp	55
	-6.470	6VW1	*SARS-CoV-2* RBD	
	-5.856	5MIM	Human Furin protease	

Catechin	-10.50	6VSB	S protein of SARS-CoV2	56
	-8.9	1R42	ACE2 receptor	
	-9.1	6LZG	RBD/ACE2- complex	

3.1.2. Docking Molecular for SARS-CoV-2.

Molecular docking generally consisted to involve docking small molecules to a known protein structure. This technology was considered to be the basic method and main strategy for drug discovery or guiding the synthesis of optimal molecular structures with biological activity. It allows users to simulate interactions between chemical species and proteins at the atomic level, thereby describing the position and conformation of the interaction of the species with the target protein and elucidating the fundamental mechanisms underlying the regulation of biological processes[57].

In this part of our investigation, we reported the molecular docking of the 12 (+)-catechin derivates designed set of molecules with the reference drug Narlaprevir [58], in the active site of the 3D structures protein, including 3CLpro/Mpro (*7JYC*), Furin (*6HZD*), and the ACE2 receptor (*6M0J*). The binding energies are represented in table 1 and the 2D interactions were illustrated in figure S2 in supporting information.

Docking scores were used to compare the best biological responses (Ligand-protein interaction) with the Narlaprevir reference and the base molecule: (+)-catechin. Compounds **2a-1** showed binding energies ranging from -7.4 to -9.2 kcal/mol, -8 to -10.1 kcal/mol, and -7.6 to -9.6 kcal/mol against 3CLpro/Mpro, ACE2, and Furin respectively. The molecular structures **2a**, **2l, 2f,** and **2i** showed good affinity with the protein target 3CLpro/Mpro, the compounds **2l,** and **2f** for the ACE2 receptor and finally all compounds except compound **2j** for the in Furin receptor.

Table 3: Molecular docking score against *SARS-CoV-2* proteins, in bold most active compounds compared to references drug.

Compounds	**Docking score(kcal/mol)**		
	7JYC	***6M0J***	***6HZD***
(+)-Catechin (1)	-8,1	-7,6	-8
2a	-8,2	-8,5	-9
2b	-7,9	-8	-8,5
2c	-7,5	-7,9	-8,3
2d	-7,6	-8	-8,2
2e	-7,6	-8,8	-9,1
2f	-8,8	-9	-10,1
2g	-7,4	-7,8	-8,3
2h	-8	-7,9	-8,1
2i	-7,9	-7,8	-8,1
2j	-7,7	-7,9	-8
2k	-9,2	-9,5	-9,5
2l	-8,5	-9,6	-10,1
Narlaprevir	**-7,7**	**-8,9**	**-7,8**

- *Molecular docking against 3CL Mpro (7JYC).*

The compounds **2a**, **2l**, **2f**, and **2k** presented significant scores -8.2, -8.5, -8.8, and -9.2 kcal/mol respectively compared to the Narlaprevir (-7.7 kcal/mol), and the (+)-catechin (**1**) (-8.1 kcal/mol). In comparison, the result obtained for the initial (+)-catechin **(1)** showed a very interesting Binding Energy value compared to other target proteins responsible for *SARS-CoV-2* such as 3CLpro/Mpro (PDB ID: *6LUZ*) with binding energy -7.240 kcal/mol[54] and *SARS-CoV-2* (Main Protease PDB ID: *5R84*) with binding energy -7.677 kcal/mol [55] (Table 2).

Compound **2a** had four hydrogen bonds with amino acid residues GLN192, GLU166, THR190, and MET165, and three π-Alkyl bonds with amino acid residues PRO168, MET165, and LEU167. **2l** compound formed three hydrogen bonds with GLU189, THR190, and MET165, and three π-Alkyl bonds with CYS145, MET165, and LEU167, π-orbital, and an electrostatic positive interaction with residue HIS41. Furthermore, the highest-scored compound **2k** did bind at active sites with two hydrogen bonds formed with amino acid HIS41, and GLU166, π-Alkyl interactions with residues MET165, PRO168, and ALA191, two alkyl interaction with MET165, and LEU167, π-sigma interaction with MET49, π-sulfur interaction with CYS145 and finally two amide interactions with residues THR190, and ALA191 (Figure 1).We can state that the compound **2k** seems to be the more effective against the 3CLpro/Mpro variant with a high score of -9.2 kcal/mol, and followed by **2f**, **2l**, and **2a**.

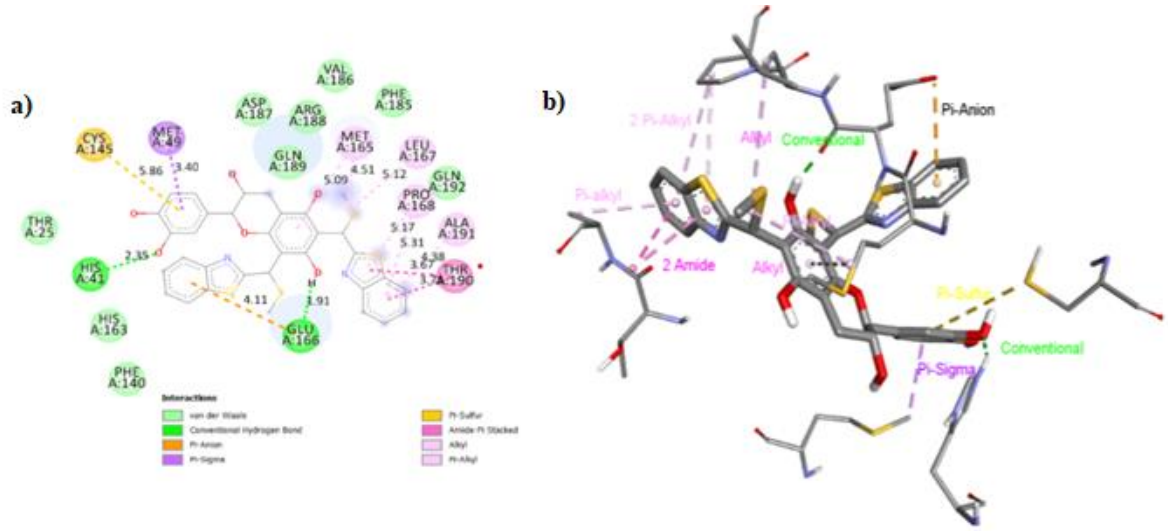

Figure 1 : (**a**) 2D and (**b**) 3D interactions visualization of the **2k** compound with receptor 3CLpro/Mpro.

- Molecular docking against ACE2 protein (6M0J).

Proceeding to the next protein, it was known that the virus enters the host cell by binding the viral spike glycoprotein to the host receptor, angiotensin converting enzyme 2 (ACE2) [59] therefore (*6M0J*) seems to be a biologically meaningful receptor. We found that the compounds **2l, 2k,** and **2f** had a negative docking score higher than the reference drugs with a score of -9.6, and -9.0 kcal/mol respectively (Table 3). They both (**2l** and **2f**) binded with hydrogen bonds with GLU406, alkyl bonds with residue ALA413, and LEU410, and π-Alkyl interactions with LEU370, and MET366. Additionally, the compound **2l** binds with THR445 and ASN290 to establish other hydrogen bond interactions. Compound **2k** also showed several types of bond with the protein: hydrogen bond of 1.86 Å with residue ALA348, bond π-π stacked with the residue PHE40, bond π-anion with the residue GLU402 and finally a bond π-sulfur with the residue HIS401. By our results, **2l** had proven to be more effective than **2k** and **2f**.

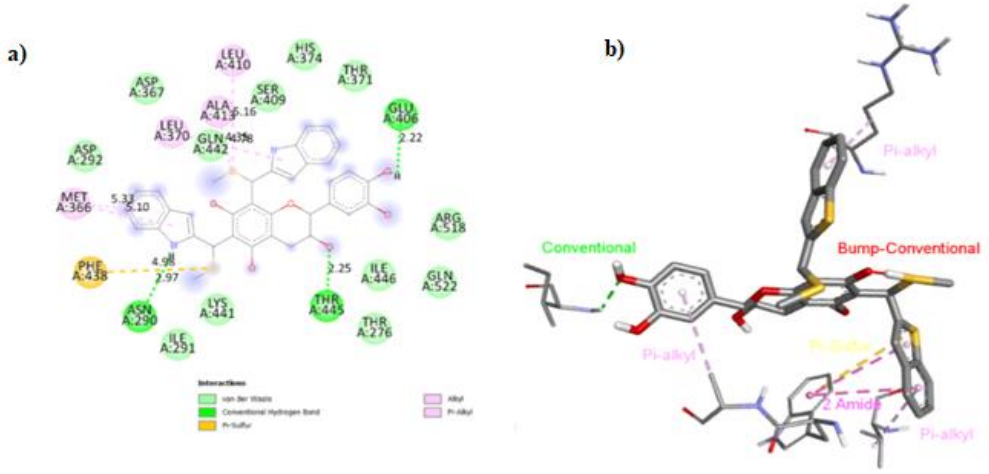

Figure 2: (**a**) 2D and (**b**) 3D interactions visualization of the **2l** compound with ACE2 receptor.

- *Molecular docking against furin in complex with the cyclic inhibitor c [glutaryl-Arg-Arg-Arg-Lys]-Arg-4-Amba (6HZD).*

Among the studied compounds, it was found that they have greater scores than the references with binding energy ≤ -8kcal/mol. The most important interactions such as hydrogen bonds, π-Alkyl, and electrostatic bonds, occurred between the ligand and the protein residues. Using the highest scores ≤ -8.5 kcal/mol, we chosed the top six compounds which are **2f**, **2l**, **2k**, **2e**, **2a**, and **2b** against the furin receptor respectively.

Compound **2f** formed a hydrogen bond with amino acid ILE312, π-alkyl bonds with ARG268, VAL263, and ALA532, and finally π-orbital bonds, π-sulfur bond with TRP531. Furthermore, compound **2k** was found to bind at the active site with TYR313 and GLN488 with two hydrogen bonds, two π-anion bonds with GLU271, four π-alkyl bonds with PRO266, VAL263, ARG268, and ILE12, alkyl bonds with ALA267, π-orbital bond with TRP531 and finally π-sulfur bond with TRP531. Interestingly, compound **2e** and **2a** formed hydrogen bonds with amino acid residues ILE312, GLY307, SER311, PRO266, ASP264, GLY265, GLN488, hydrophobic interactions with VAL263, TRP531, ALA267, ARG268, and ALA532, and electrostatic π-anion interactions with SER311, and GLU27. While compound **2b**, showed hydrogen bonds with VAL263, π-alkyl bonds with ALA532, and ARG268, π-orbital bond withTRP531, and π-anion bond with GLU271. Consistent with our results, compound **2f** and **2l** are both the most potent against the furin receptor, followed by compounds **2e**, **2a**, and **2b**.

The selected compounds could represent the starting point for a new class of inhibitors that may have advantages for the *SARS-CoV-2* disease. The compound **2l** has shown multi-target activity against 3CLMpro and Furin. Also, compound **2k** was noticed to have an action toward two varieties of targeted protein 3CLMpro and ACE2. Finally, compound **2f** has shown an inhibitory activity toward Furin and ACE2.

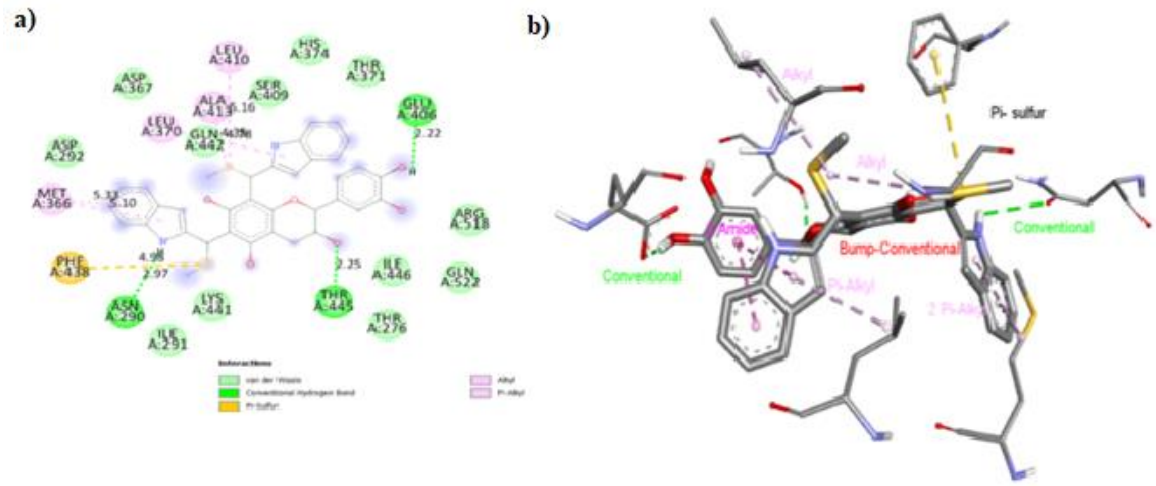

Figure 3: (**a**) 2D and (**b**) 3D interactions visualization of the **2l** compound with Furin receptor.

3.1. Bibliographic study of catechin and its derivatives against plasmodium falciparum by In silico.

The *In silico* studies concerning the anti-malarial activity of catechin and its derivatives are much less than those concerning the anti-*SARS-CoV-2* activity of these molecules. However, on three targets tested, a very good ligand-target affinity is observed for catechin derivatives (Table 4). These derivatives are natural compounds and it would be interesting to compare them to our semi-synthetic compounds.

Table 4: Study comparison carried out by *In silico* for catechin and its derivatives against anti-*plasmodium*.

Name of compound	Binding Energy Kcal/mol	PDB ID	Targed Protein	References
(+)-catechin	-7.40	*3VI2 Chain A*	*Plasmodium falciparum* orotidine 5'-monophosphate decarboxylase (PfOMPDC)	60
Epigallocatechin-3-gallate	-18	*1NHG*	*Plasmodium falciparum* enoyl-acyl carrier protein reductase (PfENR)	61
Epicatechin-gallate	-15.27			
Epigallocatechin	-12.31			
Catechin-gallate	-95.40	*1CET*	Lactate dehydrogenase	62

3.2. Docking Molecular for malaria.

The results showed in table 5, indicates that all derivative compounds have a binding affinity value between -6.3 and -7.3 kcal/mol, while the binding affinity value obtained for the references: Artesunate and the (+)-catechin (**1**) are -6.5 and -6.6 kcal/mol respectively. The representation of *2D*-interactions obtained for the (+)-catechin derivates are presented in figure S1 (Supporting information). Compounds **2b** and **2h** gave a binding energy almost equal to that Artesunate -6.5 kcal/mol. However, the other (+)-catechin derivatives **2c**, **2g**, **2i,** and **2j** gave binding energy values lower than the reference values of -6.3 kcal/mol and -6.4 kcal/mol for **2c**, **2i**, and **2j**.

Therefore, we could confirm that the designed compounds (**2a, 2e, 2f, 2k**, and **2l**) with binding energy values ≤ -6.5 kcal/mol (Artesunate) were most stable within the pocket site of the PfAMA1 protein. Furthermore, we observed that selected compounds form hydrogen bonds, hydrophobic interactions and electrostatic interactions. By visualizing molecular interaction (Figure S1, Supporting Information), molecule **2a** formed two hydrogen bonds with LYS235 and an H-donor bond with ILE18, a π-Alkyl bond with VAL208, two alkyl bonds with ARG219 and LEU211,π-cation interaction with ARG219, attractive positive charge with ASP296at a distance of 2.80 Å, 2.53 Å, 2.62 Å, 5.04 Å, 5.17 Å, 5.40 Å, 4.12 Å, and 4.23 Å respectively. Moreover, **2l** have also formed various interactions, including three H-donor bonds with ASN205, ARG219, and MET16 at a distance of 2.21 Å, 2.62 Å, and 2.40 Å respectively, π-sigma bond with VAL208 at a distance of 3.81 Å, Alkyl bond with LEU211 at a distance of 4.58 Å, and π-cation interaction with ARG219, attractive positive charge with ASP296 at a distance of 4.27 Å, and 4.42 Å respectively. Likewise, compound **2f** created a variety of interactions, including three hydrogen bonds with TYR175, TYR142, and MET273 at a distance of 2.49, 2.86 , and 2.55 Å respectively, four π-Alkyl bonds with PRO7, ALA3, and LEU211 at a distance of 5.46, 4.56, 4.67, and 4.68 Å respectively, π-sulfur bond with TYR142 at a distance of 2.49 Å.

We can conclude from the docking analysis, that the binding of the molecules to the receptor will transform the target protein's state into a functional state, causing a reaction that will lead to the inhibition of the *Plasmodium* disease. Also, the designed molecules demonstrated strong receptor-binding bonds toward the PfAMA1 protein. Compounds **2f** and **2l** prove to be the best inhibitors against *Plasmodium falciparum*.

Table 5: Interaction between the (+)-catechin derivates and the targeted receptor PfAMA1 (PDB ID: *3SRJ*).

Ligands	Receptor	Docking score (kcal/mol)	Hydrogen-Binding interaction	Hydrophobic interaction	Other interaction: Electrostatics and unfavorable bonds ()
Artesunate	PfAMA1 (PDB ID: 3SRJ)	-6,5	ASN205 LYS235	-	-
1		-6.6	GLY179 SER161 LYS177 ASN160	CYS275	(SER272) ASP178
2a		-6,6	LYS235 ILE18	ARG219 LEU211 VAL208	ASP296 ARG219
2b		-6.5	ASN205 ARG15 MET16 ARG219 LYS292 ASP296 ASN 223	VAL208	ARG219
2c		-6,3	ASN205 ARG15	VAL208 LEU211 ARG219	(LYS235) ARG219
2d		-6,4	MET16 ASN293 ASN223	VAL208	ASP296 ARG219
2e		-6,7	PHE5 TYR175 LYS177 LEU8	ALA138 ALA3 PRO7 LEU8	-
2f		-7,3	TYR175 TYR142 MET273	PRO7ALA3 MET273	TYR142
2g		-6,4	ARG15 MET16 ASN223	LEU221 ARG219 VAL208	ASP296 ARG219
2h		-6,5	2MET16	VAL208 LEU211 ARG219	ASP296 ARG219
2i		-6,3	ASN2052 LYS235	LEU221 ARG219 VAL208	ASP296 ARG219 (LYS235)
2j		-6,3	MET273 PHE5 GLY172	-	LYS177
2k		-6,8	ARG219 ILE18 ARG219	VAL208	ARG219 (MET16)
2l		-7,2	ASN205 ARG219 MET16	VAL208 LEU211	ASP296 ARG219

3.3. ADMET analysis of catechin derivates.

3.3.1. Prediction of ADME.

ADMET (Absorption, Distribution, Metabolism, Excretion, and Toxicity) is an important method in drug design and development processes. The drug-like properties including molecular weight (MW) (< 500), lipophilicity (< 4.15), Hydrogen Bond Acceptor (HBA) (< 10), Hydrogen Bond Donor (HBD) (< 5), Topological Polar Surface Area (TPSA) (<140 $Å^2$), water-solubility (Log S), pharmacokinetics (gastrointestinal absorption, Blood–Brain Barrier, and Permeability) were calculated using Swiss ADME, and toxicity (mutagenic, tumorigenic, irritant, and reproductive effect) have been performed by using Protox online server [63].

The molecular weight of all (+)-catechin derivates aren't in the range of drug-likeness properties (Mw< 500 g. mol^{-1}), except (+)-catechin (**1**) with Mw = 290 g. mol^{-1}. As shown in tables 6 and 7, among the 12 (+)-catechin derivatives, **1**, **2b-c**, **2e,** and **2g-k** compounds showed higher bioavailability (> 0.50) unlike to the remain compounds **2a**, **2d**, **2f**, and **2l** (Bioavailability score = 0.17) to generate main therapeutic agents against *SARS-CoV-2* and/or anti-malarial (Table 6 and 7). The Log S number represents the drug's water solubility. The solubility of all evaluated compounds ranged from -2.24 to -8.98 mol/L. Compounds **2a**, **2c**, **2e-f,** and **2k-l** showed low water solubility, and the other compounds **2b**, **2d**, **2g**, and **2i-j** have moderate solubility, unlike the base molecule which exhibits good solubility with Log S -2.24 mol/L (Table 6 and 7). According to ADMET characteristics, all catechin derivates **2a-l** have a low rate of human GI absorption, whereas only (+)-catechin (**1**) have a high rate of human GI absorption and have a good rate drug gable properties (Table 7).

Table 6: *Results of ADME and drug-likeness properties of (+)-catechin derivates.*

Compounds	Mw (g.mol^{-1})	MLog P	HBA	HBD	Rot N	TPSA (A^2)	Solubility	Log S (mol/l)	Lipinski	Veber	Bioavailability
1	290.27	*0.24*	*6*	*5*	*1*	110.38	*Soluble*	*-2.24*	*Yes: 0 violation*	*Yes: 0 violation*	*0.55*
2a	*594.70*	*3.86*	*8*	*7*	*7*	*201.44*	*Poorly*	*-6.64*	*No: 2 violation*	*No: 1 violation*	*0.17*
2b	564.67	3.30	*8*	*5*	*7*	*186.76*	*Moderately*	*-5.58*	*Yes: 1 violation*	*No: 1 violation*	*0.55*
2c	*574.75*	*4.78*	*6*	*5*	*7*	*217.46*	*Poorly*	*-6.62*	*Yes: 1 violation*	*No: 1 violation*	*0.55*
2d	*540.65*	*3.17*	*6*	*7*	*7*	*192.56*	*Moderately*	*-5.28*	*No: 2 violation*	*No: 1 violation*	*0.17*
2e	*614.77*	*5.72*	*6*	*5*	*9*	*160.98*	*Poorly*	*-7.87*	*Yes: 1 violation*	*No: 1 violation*	*0.55*
2f	*674.87*	*6.66*	*5*	*6*	*7*	*217.46*	*Poorly*	*-8.98*	*No: 2 violation*	*No: 1 violation*	*0.17*
2g	564.67	3.30	*8*	*5*	*7*	*186.76*	*Moderately*	*-5.58*	*Yes: 1 violation*	*No: 1 violation*	*0.55*
2h	*568.70*	*3.05*	*6*	*5*	*7*	*170.84*	*Moderately*	*-5.38*	*Yes: 1 violation*	*No: 1 violation*	*0.55*
2i	*576.73*	*3.54*	*8*	*5*	*7*	*243.24*	*Moderately*	*-5.81*	*Yes: 1 violation*	*No: 1 violation*	*0.55*
2j	*544.60*	*2.35*	*10*	*5*	*7*	*213.04*	*Moderately*	*-4.84*	*Yes: 1 violation*	*No: 1 violation*	*0.55*
2k	*676.85*	*5.46*	*8*	*5*	*7*	*243.24*	*Poorly*	*-8.28*	*Yes: 1 violation*	*No: 1 violation*	*0.55*
2l	*640.77*	*5.08*	*6*	*7*	*7*	*192.56*	*Poorly*	*7.64*	*No: 2 violation*	*No: 1 violation*	*0.17*
Artesunate	*384.42*	*2.22*	*8*	*1*	*5*	*186.37*	*Soluble*	*-3.08*	*Yes: 0 violation*	*Yes*	*0.56*
Narlaprevir	*709.98*	*3.74*	*9*	*5*	*16*	*183.63*	*Poorly*	*-6.86*	*No: 2 violation*	*No: 2 violation*	*0.17*

Table 7: Continuation of table 6.

Compounds	GI	BBB	Cyp1A2	Cyp2C19	Cyp2C9	Cyp2D6	Cyp3A4	Log Kp Skin permeation (cm/s)	PAINS Alert
1	*High*	*No*	*No*	*No*	*No*	*No*	*No*	*-7.82*	1 Alert Catechol_A
2a	*Low*	*No*	*No*	*No*	*No*	*No*	*Yes*	*-6.38*	1 Alert Catechol_A
2b	*Low*	*No*	*No*	*No*	*No*	*No*	*Yes*	*-7.22*	1 Alert Catechol_A
2c	*Low*	*No*	*No*	*No*	*Yes*	*No*	*Yes*	*-6.16*	1 Alert Catechol_A
2d	*Low*	*No*	*No*	*No*	*No*	*No*	*Yes*	*-7.22*	1 Alert Catechol_A
2e	*Low*	*No*	*No*	*No*	*No*	*No*	*Yes*	*-5.09*	1 Alert Catechol_A
2f	*Low*	*No*	*No*	*No*	*No*	*No*	*Yes*	*-4.87*	1 Alert Catechol_A
2g	*Low*	*No*	*No*	*No*	*No*	*No*	*Yes*	*-7.22*	1 Alert Catechol_A
2h	*Low*	*No*	*No*	*No*	*No*	*No*	*Yes*	*-7.45*	1 Alert Catechol_A
2i	*Low*	*No*	*No*	*No*	*Yes*	*No*	*Yes*	*-7.09*	1 Alert Catechol_A
2j	*Low*	*No*	*No*	*No*	*No*	*No*	*Yes*	*-7.77*	1 Alert Catechol_A
2k	*Low*	*No*	*No*	*No*	*No*	*No*	*Yes*	*-5.68*	1 Alert Catechol_A
2l	*Low*	*No*	*No*	*No*	*No*	*No*	*Yes*	*-7.64*	1 Alert Catechol_A
Artesunate	*High*	*No*	*No*	*No*	*No*	*No*	*No*	*-7.31*	*0 Alert*
Narlaprevir	*Low*	*No*	*No*	*No*	*No*	*No*	*Yes*	*-6.49*	*0 Alert*

MW: Molecular Weight, **HBA**: Hydrogen Bond Acceptor, **HBD**: Hydrogen Bond Donor, **TPSA**: Topological Polar Surface Area, **MLogP** = Lipophilicity, **LogS**:Water Solubility, **GI**: Gastrointestinal Absorption, **BBB**: Blood-Brain Barrier.

3.3.2. Catechin and derivates toxicity.

The purpose of the toxicity study is to see if the catechin derivatives showed adverse drug effects, such as hepatotoxicity, carcinogenicity, mutagenicity and cytotoxicity. It is essential to highlight this series of compounds **1** and **2a-l** as being candidates taking into account the different stages of pharmacokinetic studies carried out with the calculated ADMET parameters. Table 4 illustrates the results obtained using the ProTox II web server to assess the toxicological class of compounds. (+)-catechin showed no toxicity, the LD50 value was too high (10000 mg. Kg^{-1}, class 6). This toxicological profile has been altered with the structural modification of the (+)-catechin molecular framework. All compounds were considered inactive in different toxicity categories, except compounds **2a**, **2i,** and **2k** which showed toxicological activity in the liver (Hepatotoxicity). This study also allowed us to determine the theoretical LD50 value, which represents the dose at which 50% of the tested organisms die after exposure to the compound The LD50 value of compound **2a** was 1190 mg. Kg^{-1} compared with other compound **2b-l** (LD50 = 2500 mg. Kg^{-1}). From this, it can be concluded that class 5 compounds with high LD50 values (= 2500 mg. Kg^{-1}) are considered to be less toxic (Table 8).

Table 8: Toxicological properties of (+)-catechin derivates.

Ligands	Hepatotoxicity	Carcinogenicity	Mutagenicity	Cytotoxicity	LD50 (mg.Kg^{-1})	Class
1	Inactive	Inactive	Inactive	Inactive	10000	6
2a	**Active**	Inactive	Inactive	Inactive	1190	4
2b	Inactive	Inactive	Inactive	Inactive	2500	5
2c	Inactive	Inactive	Inactive	Inactive	2500	5
2d	Inactive	Inactive	Inactive	Inactive	2500	5
2e	Inactive	Inactive	Inactive	Inactive	2500	5
2f	Inactive	Inactive	Inactive	Inactive	2500	5
2g	Inactive	Inactive	Inactive	Inactive	2500	5
2h	Inactive	Inactive	Inactive	Inactive	2500	5
2i	**Active**	Inactive	Inactive	Inactive	2500	5
2j	Inactive	Inactive	Inactive	Inactive	2500	5
2k	**Active**	Inactive	Inactive	Inactive	2500	5
2l	Inactive	Inactive	Inactive	Inactive	2500	5

3.4. Molecular Dynamic Simulation.

After the dynamics simulations, we analyzed the outcomes of each system by assessing the parameters (RMSD, RMSF, and interaction diagram) calculated by the MD trajectories. Figure 4 depicts the RMSD of the Cα protein and the RMSD of the ligand as a function of simulation time for both simulated systems. Both complexes *3SRJ*-**2f** (*Anti-plasmodium activity*) and *6HZD*-**2l** (Anti-*SARS-CoV-2* activity) exhibited an average RMSD value of 1.5 and 2.4 Å respectively all across the simulation.

The outcomes of the dynamic for the first complex *3SRJ*-**2f** illustrated in figure 4A demonstrate that the Root Mean Square Deviation (RMSD) found equilibrium at 40 ns after an initial oscillation. The system then stayed stable throughout the MD simulation, showing that it progressed to a more perfect equilibrium state than the starting structure. While the RMSD plot for the second complex *6HZD*-**2l** (Figure 4B) indicates a significant divergence during the first part of the experiment, but eventually stabilizes between 40 and 60 ns then fluctuate at 70 ns and system gets equilibrated after 75 ns.

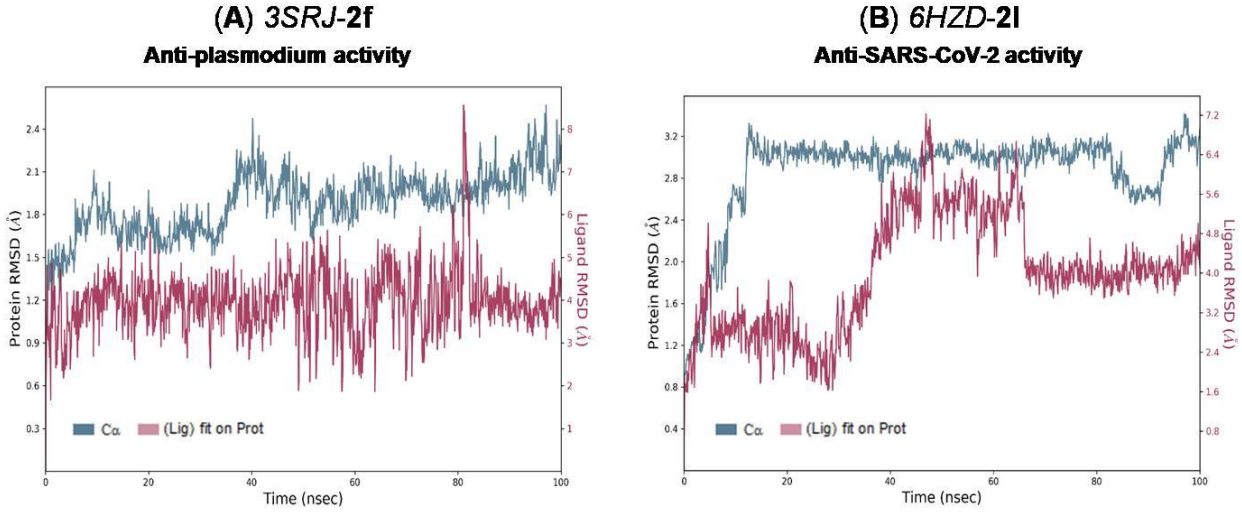

Figure 4: RMSD plot for complexes (**A**) *3SRJ*-**2f** and (**B**) *6HZD*-**2l**.

We also investigated the Root Mean Square Fluctuation (RMSF) values of each backbone atom in both complexes to analyze how much a specific residue varies during the simulation [47], (Figure 5). The peaks on both graphics represent the portions of the protein that fluctuate the greatest during the simulation. For the first complex *3SRJ*-**2f** (Figure 5A), it is shown that in all complexes, the variation occurred in the C-terminal residues of proteins, and in residue Ser272 (4.5 Å), since they are positioned in the inactive regions of the protein, these residues are not engaged. In contrast, important active site residues such as Thy175, Lys177 have smaller RMSF fluctuations of less than 2 Å, which could be related to the formation of more hydrogen-bonding interactions for greater ligand stability with the *3SRJ* protein indicating that the combination is stable. The second complex *6HZD*-**2l,** had an average RMSF of 1.2 Å (Figure 5B). Moreover, most of the amino acid residues in the *6HZD*-**2l** complex are smaller than 2 Å in length. Overall, the RMSF figure 5 shows that there are no substantial changes in residual fluctuations when **2l** is bound to *6HZD*.

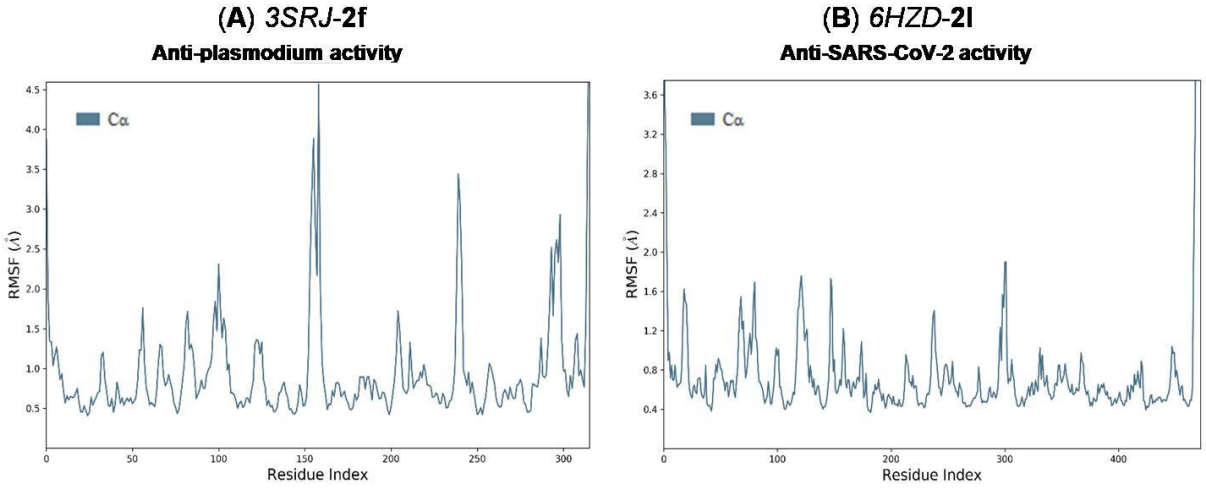

Figure 5: RMSF plot for complexes (**A**) *3SRJ*-**2f** and (**B**) *6HZD*-**2l**.

The interaction of **2l** with *6HZD* produced during the simulation (Figure 6B) revealed that compound **2l** established multiple interactions with distinct substrates in the binding sites, including hydrogen bonds, hydrophobic interactions, ionic interactions, and water bridges. Pro266, Glu271, Asn310, Gln488, Trp531, and Ala532 were the amino acid residues implicated in the stability of the *6HZD*-**2l** complex during the simulation, and they formed mainly two types of interactions: hydrogen bonds and water bridges. While the main observed interaction between *3SRJ* and **2f** (Figure 6A), are hydrogen bonds and hydrophobic interactions with Thyr175, Lys177, Ser272, Met273, and Phe5.

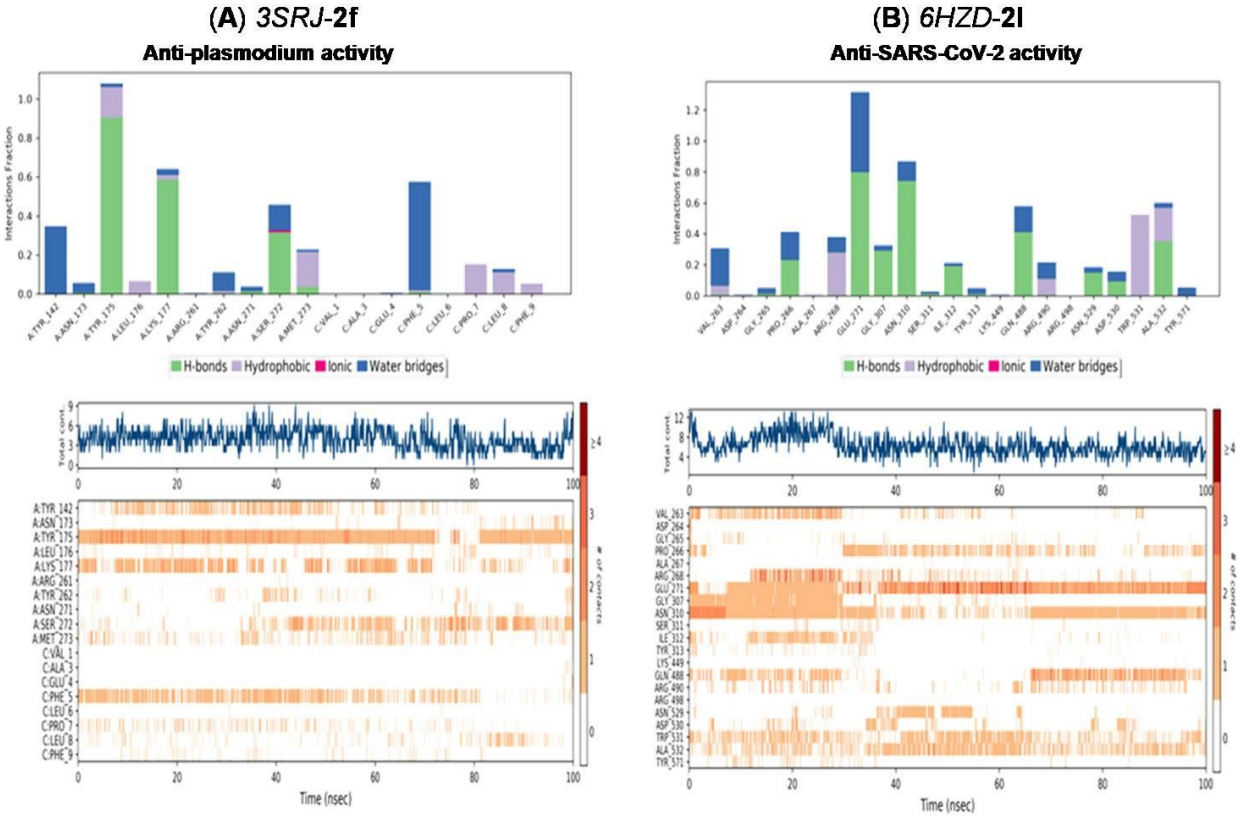

Figure 6: Protein ligands interactions for both complexes (**A**) *3SRJ*-**2f** and (**B**) *6HZD*-**2l**.

4. CONCLUSION

The result showed a clearly promising and encouraging track for the hemisynthesis of (+)-catechin for the anti-*SARS-CoV-2* and anti-malarial activities. The theoretical simulation gave an orientation or a priority for certain compounds among the 12 catechin-aldehyde with (*R, R*) or (*S, S*) conformation, studied for the experimental suite of this project. Most structures presented a good affinity with the target protein responsible for *SARS-CoV-2* and/or *Plasmodium falciparum,* compared to the references used Narlaprevir and Artesunate respectively. The evaluation of the toxicity of these compounds **2a-l** revealed that the series didn't show toxicity except for compounds **2a**, **2i**, and **2k** which exhibit hepatotoxicity.

Compounds **2f** and **2l** are the best candidates for anti-malarial and anti-*SARS-CoV-2* activity respectively among the series of compounds. Molecular dynamics also showed the good stability of complexes formed of *3SRJ*-**2f** and *6HZD*-**2l** via Ligand-protein intermolecular binding at 100 ns. Subsequently, the hemisynthesis of these two compounds **2f** and **2l** are the priority, followed by the rest of the catechin-aldehyde series.

Conflict of Interest

The authors declare that they have no conflict of interest.

Credit authorship contribution statement

Ahmed Said Mohamed and **Samir Chtita**: Conceptualization, Methodology, Supervision, Data curation, Writing – review & editing, Writing – original draft. **Imane Yamari** and **Nouh Mounadi**: Conceptualization, Writing – original draft. **Abdirahman Elmi**: Writing – original draft. **Mohammed Bouachrine** and **Hanane Zaki**: Visualization, Investigation, Validation. **Ahmed Said Mohamed** and **Samir Chtita**: Conceptualization, Methodology, Software, Supervision.

Acknowledgements

This research was funded by TWAS-UNESCO and Sida 21-029 RG/CHE/AF/AC_I 2021-2023. Furthermore, all the authors of the manuscript also thank and acknowledge their respective Universities and Institutes.

REFERENCES

1. Acharya PP, Genwali GR, Rajbhandari M. Isolation of Catechin from Acacia catechu Willdenow Estimation of Total Flavonoid Content in Camellia Sinensis Kuntze and Camellia Sinensis Kuntze Var. Assamica Collected from Different Geographical Region and Their Antioxidant Activities. Scientific World. 2013;11(11):32-36. https://doi.org/10.3126/sw.v11i11.8549

2. Elmi A, Spina R, Risler A, et al. Evaluation of Antioxidant and Antibacterial Activities, Cytotoxicity of Acacia seyal Del Bark Extracts and Isolated Compounds. Molecules. 2020;25(10):2392. https://doi.org/10.3390/molecules25102392 PMid:32455580 PMCid:PMC7288156

3. Grzesik M, Naparło K, Bartosz G, Sadowska-Bartosz I. Antioxidant properties of catechins: Comparison with other antioxidants. Food Chemistry. 2018;241:480-492. https://doi.org/10.1016/j.foodchem.2017.08.117 PMid:28958556

4. Higdon JV, Frei B. Tea Catechins and Polyphenols: Health Effects, Metabolism, and Antioxidant Functions. Critical Reviews in Food Science and Nutrition. 2003;43(1):89-143. https://doi.org/10.1080/10408690390826464 PMid:12587987

5. Nakao M, Takio S, Ono K. Alkyl peroxyl radical-scavenging activity of catechins. Phytochemistry. 1998;49(8):2379-2382. https://doi.org/10.1016/S0031-9422(98)00333-1 PMid:9887529

6. Shirakami Y, Shimizu M. Possible Mechanisms of Green Tea and Its Constituents against Cancer. Molecules. 2018;23(9):2284. https://doi.org/10.3390/molecules23092284 PMid:30205425 PMCid:PMC6225266

7. Zaveri NT. Green tea and its polyphenolic catechins: Medicinal uses in cancer and noncancer applications. Life Sciences. 2006;78(18):2073-2080. https://doi.org/10.1016/j.lfs.2005.12.006 PMid:16445946

8. Weyant MJ, Carothers AM, Dannenberg AJ, Bertagnolli MM. (+)-Catechin Inhibits Intestinal Tumor Formation and Suppresses Focal Adhesion Kinase Activation in the Min/+ Mouse1. Cancer Research. 2001;61(1):118-125.

9. Kemal T, Feyisa K, Bisrat D, Asres K. In Vivo Antimalarial Activity of the Leaf Extract of Osyris quadripartita Salzm. ex Decne and Its Major Compound (-) Catechin. Journal of Tropical Medicine. 2022;2022:e3391216. https://doi.org/10.1155/2022/3391216 PMid:36249737 PMCid:PMC9568338

10. Vyas VK, Bhati S, Patel S, Ghate M. Structure- and ligand-based drug design methods for the modeling of antimalarial agents: a review of updates from 2012 onwards. Journal of Biomolecular Structure and Dynamics. 2022;40(20):10481-10506. https://doi.org/10.1080/07391102.2021.1932598 PMid:34129805

11. Saleh Abu-Lafi, Mutaz Akkawi, Fuad Al-Rimawi, Qassem Abu-Remeleh, Pierre Lutgen. Morin, quercetin, catechin and quercitrin as novel natural antimalarial candidates. Pharm Pharmacol Int J. 2020;8(3):184-190. https://doi.org/10.15406/ppij.2020.08.00295

12. Moelyadi F, Utami PD, Dikman IM. Inhibitory Effect of Active Substances of Lollyfish (Holothuria atra) Against the Development of Plasmodium falciparum Based on In Silico Study. ILMU KELAUTAN: Indonesian Journal of Marine Sciences. 2020;25(4):135-142. https://doi.org/10.14710/ik.ijms.25.4.135-142

13. Abdulah R, Suradji EW, Subarnas A, et al. Catechin Isolated from Garcinia celebica Leaves Inhibit Plasmodium falciparum Growth through the Induction of Oxidative Stress. Pharmacogn Mag. 2017;13(Suppl 2):S301-S305. https://doi.org/10.4103/pm.pm_571_16 PMid:28808396 PMCid:PMC5538170

14. Chtita S, Fouedjou RT, Belaidi S, et al. In silico investigation of phytoconstituents from Cameroonian medicinal plants towards COVID-19 treatment. Struct Chem. 2022;33(5):1799-1813. https://doi.org/10.1007/s11224-022-01939-7 PMid:35505923 PMCid:PMC9051495

15. Jha RK, Khan RJ, Parthiban A, et al. Identifying the natural compound Catechin from tropical mangrove plants as a potential lead candidate against 3CLpro from SARS-CoV-2: An integrated in silico approach. Journal of Biomolecular Structure and Dynamics. 2022;40(24):13392-13411. https://doi.org/10.1080/07391102.2021.1988710 PMid:34644249

16. Ouassaf M, Belaidi S, Chtita S, Lanez T, Abul Qais F, Md Amiruddin H. Combined molecular docking and dynamics simulations studies of natural compounds as potent inhibitors against SARS-CoV-2 main protease. Journal of Biomolecular Structure and Dynamics. 2022;40(21):11264-11273. https://doi.org/10.1080/07391102.2021.1957712 PMid:34315340

17. Sannella AR, Messori L, Casini A, et al. Antimalarial properties of green tea. Biochemical and Biophysical Research Communications. 2007;353(1):177-181. https://doi.org/10.1016/j.bbrc.2006.12.005 PMid:17174271

18. Budiman I, Tjokropranoto R, Widowati W, Rahardja F, Maesaroh M, Fauziah N. Antioxidant and Anti-malarial Properties of Catechins. Journal of Advances in Medicine and Medical Research. Published online 2015:895-902. https://doi.org/10.9734/BJMMR/2015/11451 PMid:26099036

19. Cucinotta D, Vanelli M. WHO Declares COVID-19 a Pandemic. Acta Biomed. 2020;91(1):157-160. doi:10.23750/abm.v91i1.9397

20. Duzgun Z, Kural BV, Orem A, Yildiz I. In silico investigation of the interactions of certain drugs proposed for the treatment of Covid-

19 with the paraoxonase-1. Journal of Biomolecular Structure and Dynamics. 2023;41(3):884-896. https://doi.org/10.1080/07391102.2021.2014971 PMid:34895069

21. de Oliveira OV, Cristina Andreazza Costa M, Marques da Costa R, Giordano Viegas R, Paluch AS, Miguel Castro Ferreira M. Traditional herbal compounds as candidates to inhibit the SARS-CoV-2 main protease: an in silico study. Journal of Biomolecular Structure and Dynamics. 2023;41(5):1603-1616. https://doi.org/10.1080/07391102.2021.2023646 PMid:36719113

22. Chtita S, Belhassan A, Bakhouch M, et al. QSAR study of unsymmetrical aromatic disulfides as potent avian SARS-CoV main protease inhibitors using quantum chemical descriptors and statistical methods. Chemometrics and Intelligent Laboratory Systems. 2021;210:104266. https://doi.org/10.1016/j.chemolab.2021.104266 PMid:33558778 PMCid:PMC7857023

23. Ngwa W, Kumar R, Thompson D, et al. Potential of Flavonoid-Inspired Phytomedicines against COVID-19. Molecules. 2020;25(11):2707. https://doi.org/10.3390/molecules25112707 PMid:32545268 PMCid:PMC7321405

24. Ansari WA, Khan MA, Rizvi F, et al. Computational Screening of Plant-Derived Natural Products against SARS-CoV-2 Variants. Future Pharmacology. 2022;2(4):558-578. https://doi.org/10.3390/futurepharmacol2040034

25. Diniz LRL, Elshabrawy HA, Souza MT de S, Duarte ABS, Datta S, de Sousa DP. Catechins: Therapeutic Perspectives in COVID-19-Associated Acute Kidney Injury. Molecules. 2021;26(19):5951. https://doi.org/10.3390/molecules26195951 PMid:34641495 PMCid:PMC8512361

26. Zhang Z, Zhang X, Bi K, et al. Potential protective mechanisms of green tea polyphenol EGCG against COVID-19. Trends in Food Science & Technology. 2021;114:11-24. https://doi.org/10.1016/j.tifs.2021.05.023 PMid:34054222 PMCid:PMC8146271

27. Mhatre S, Gurav N, Shah M, Patravale V. Entry-inhibitory role of catechins against SARS-CoV-2 and its UK variant. Computers in Biology and Medicine. 2021;135:104560. https://doi.org/10.1016/j.compbiomed.2021.104560 PMid:34147855 PMCid:PMC8189743

28. Shaik FB, Swarnalatha K, Mohan MC, et al. Novel antiviral effects of chloroquine, hydroxychloroquine, and green tea catechins against SARS CoV-2 main protease (Mpro) and 3C-like protease for COVID-19 treatment. Clinical Nutrition Open Science. 2022;42:62-72. https://doi.org/10.1016/j.nutos.2021.12.004 PMid:35106518 PMCid:PMC8795779

29. Andi B, Kumaran D, Kreitler DF, et al. Hepatitis C virus NS3/4A inhibitors and other drug-like compounds as covalent binders of SARS-CoV-2 main protease. Sci Rep. 2022;12(1):12197. https://doi.org/10.1038/s41598-022-15930-z PMid:35842458 PMCid:PMC9287821

30. Berman H, Henrick K, Nakamura H. Announcing the worldwide Protein Data Bank. Nat Struct Mol Biol. 2003;10(12):980-980. https://doi.org/10.1038/nsb1203-980 PMid:14634627

31. Van Lam van T, Ivanova T, Hardes K, et al. Design, Synthesis, and Characterization of Macrocyclic Inhibitors of the Proprotein Convertase Furin. ChemMedChem. 2019;14(6):673-685. https://doi.org/10.1002/cmdc.201800807 PMid:30680958

32. Lan J, Ge J, Yu J, et al. Structure of the SARS-CoV-2 spike receptor-binding domain bound to the ACE2 receptor. Nature. 2020;581(7807):215-220. https://doi.org/10.1038/s41586-020-2180-5 PMid:32225176

33. Vulliez-Le Normand B, Tonkin ML, Lamarque MH, et al. Structural and Functional Insights into the Malaria Parasite Moving Junction Complex. Phillips M, ed. PLoS Pathog. 2012;8(6):e1002755. https://doi.org/10.1371/journal.ppat.1002755 PMid:22737069 PMCid:PMC3380929

34. Kajiya K, Hojo H, Suzuki M, Nanjo F, Kumazawa S, Nakayama T. Relationship between Antibacterial Activity of (+)-Catechin Derivatives and Their Interaction with a Model Membrane. J Agric Food Chem. 2004;52(6):1514-1519. https://doi.org/10.1021/jf0350111 PMid:15030204

35. Trott O, Olson AJ. AutoDock Vina: improving the speed and accuracy of docking with a new scoring function, efficient optimization and multithreading. Journal of computational chemistry. 2010;31(2):455. https://doi.org/10.1002/jcc.21334 PMid:19499576 PMCid:PMC3041641

36. Trott O, Olson AJ. AutoDock Vina: Improving the speed and accuracy of docking with a new scoring function, efficient optimization, and multithreading. Journal of Computational Chemistry. Published online 2009:NA-NA. https://doi.org/10.1002/jcc.21334 PMid:19499576 PMCid:PMC3041641

37. Peixoto HM, Marchesini PB, de Oliveira MRF. Efficacy and safety of artesunate-mefloquine therapy for treating uncomplicated Plasmodium falciparum malaria: systematic review and meta-analysis. Transactions of The Royal Society of Tropical Medicine and Hygiene. Published online December 29, 2016. https://doi.org/10.1093/trstmh/trw077 PMid:28039388

38. ADT / AutoDockTools - AutoDock. Accessed September 18, 2021. http://autodock.scripps.edu/resources/adt

39. Hanwell MD, Curtis DE, Lonie DC, Vandermeerschd T, Zurek E, Hutchison GR. Avogadro: an advanced semantic chemical editor, visualization, and analysis platform. Journal of cheminformatics. 2012;4(1). https://doi.org/10.1186/1758-2946-4-17 PMid:22889332 PMCid:PMC3542060

40. "Free Download: BIOVIA Discovery Studio Visualizer - Dassault Systèmes." https://discover.3ds.com/discovery-studio-visualizer-download (accessed Jun. 13, 2021).

41. Ioakimidis L, Thoukydidis L, Mirza A, Naeem S, Reynisson J. Benchmarking the Reliability of QikProp. Correlation between Experimental and Predicted Values. QSAR & Combinatorial Science. 2008;27(4):445-456. https://doi.org/10.1002/qsar.200730051

42. Banerjee P, Eckert AO, Schrey AK, Preissner R. ProTox-II: a webserver for the prediction of toxicity of chemicals. Nucleic Acids Research. 2018;46(W1):W257-W263. https://doi.org/10.1093/nar/gky318 PMid:29718510 PMCid:PMC6031011

43. Roos K, Wu C, Damm W, et al. OPLS3e: Extending Force Field Coverage for Drug-Like Small Molecules. Journal of Chemical Theory and Computation. 2019;15(3):1863-1874. https://doi.org/10.1021/acs.jctc.8b01026 PMid:30768902

44. System, Maestro-Desmond Interoperability Tools, Schrödinger, New York, NY, 2021.

45. Ouassaf M, Belaidi S, Mogren Al Mogren M, Chtita S, Ullah Khan S, Thet Htar T. Combined docking methods and molecular dynamics to identify effective antiviral 2, 5-diaminobenzophenonederivatives against SARS-CoV-2. Journal of King Saud University - Science. 2021;33(2):101352. https://doi.org/10.1016/j.jksus.2021.101352 PMid:33558797 PMCid:PMC7857992

46. Nour H, Daoui O, Abchir O, ElKhattabi S, Belaidi S, Chtita S. Combined computational approaches for developing new anti-Alzheimer drug candidates: 3D-QSAR, molecular docking and molecular dynamics studies of liquiritigenin derivatives. Heliyon. 2022;8(12):e11991. https://doi.org/10.1016/j.heliyon.2022.e11991 PMid:36544815 PMCid:PMC9761610

47. Singh MB, Sharma R, Kumar D, et al. An understanding of coronavirus and exploring the molecular dynamics simulations to find promising candidates against the Mpro of nCoV to combat the COVID-19: A systematic review. Journal of Infection and Public Health. 2022;15(11):1326-1349. https://doi.org/10.1016/j.jiph.2022.10.013 PMid:36288640 PMCid:PMC9579205

48. Parrinello M, Rahman A. Polymorphic transitions in single crystals: A new molecular dynamics method. Journal of Applied Physics. 1981;52(12):7182-7190. https://doi.org/10.1063/1.328693

49. Ghosh R, Chakraborty A, Biswas A, Chowdhuri S. Evaluation of green tea polyphenols as novel corona virus (SARS CoV-2) main protease (Mpro) inhibitors - an in silico docking and molecular dynamics simulation study. J Biomol Struct Dyn. Published online June 22, 2020:1-13. https://doi.org/10.1080/07391102.2020.1779818 PMid:32568613 PMCid:PMC7332865

50. Ohishi T, Hishiki T, Baig MS, et al. Epigallocatechin gallate (EGCG) attenuates severe acute respiratory coronavirus disease 2 (SARS-CoV-2) infection by blocking the interaction of SARS-CoV-2 spike protein receptor-binding domain to human angiotensin-converting enzyme 2. PLOS ONE. 2022;17(7):e0271112. https://doi.org/10.1371/journal.pone.0271112 PMid:35830431 PMCid:PMC9278780

51. Chourasia M, Koppula PR, Battu A, Ouseph MM, Singh AK. EGCG, a Green Tea Catechin, as a Potential Therapeutic Agent for Symptomatic and Asymptomatic SARS-CoV-2 Infection. Molecules. 2021;26(5):1200. https://doi.org/10.3390/molecules26051200 PMid:33668085 PMCid:PMC7956763

52. Frengki F, Putra DP, Wahyuni FS, Khambri D, Vanda H, Sofia V. POTENTIAL ANTIVIRAL OF CATECHINS AND THEIR DERIVATIVES TO INHIBIT SARS-COV-2 RECEPTORS OF M pro PROTEIN AND SPIKE GLYCOPROTEIN IN COVID-19 THROUGH THE IN SILICO APPROACH. Jurnal Kedokteran Hewan - Indonesian Journal of Veterinary Sciences. 2020;14(3). https://doi.org/10.21157/j.ked.hewan.v14i3.16652

53. Mishra CB, Pandey P, Sharma RD, et al. Identifying the natural polyphenol catechin as a multi-targeted agent against SARS-CoV-2 for the plausible therapy of COVID-19: an integrated computational approach. Briefings in Bioinformatics. 2021;22(2):1346-1360. https://doi.org/10.1093/bib/bbaa378 PMid:33386025 PMCid:PMC7799228

54. Kashyap P, Thakur M, Singh N, et al. In Silico Evaluation of Natural Flavonoids as a Potential Inhibitor of Coronavirus Disease. Molecules. 2022;27(19):6374. https://doi.org/10.3390/molecules27196374 PMid:36234910 PMCid:PMC9572657

55. Elmi A, Sayem SAJ, Ahmed M, Abdoul-Latif F. NATURAL COMPOUNDS FROM DJIBOUTIAN MEDICINAL PLANTS AS INHIBITORS OF COVID-19 BY IN SILICO INVESTIGATIONS. International Journal of Current Pharmaceutical Research. Published online July 15, 2020:52-57. https://doi.org/10.22159/ijcpr.2020v12i4.39051

56. Jena AB, Kanungo N, Nayak V, Chainy GBN, Dandapat J. Catechin and curcumin interact with S protein of SARS-CoV2 and ACE2 of human cell membrane: insights from computational studies. Sci Rep. 2021;11(1):2043. https://doi.org/10.1038/s41598-021-81462-7 PMid:33479401 PMCid:PMC7820253

57. Martinez-Archundia M, Colin-Astudillo B, Gómez-Hernández L, Abarca-Rojano E, Correa-Basurto J. Docking analysis provide structural insights to design novel ligands that target PKM2 and HDC8 with potential use for cancer therapy. Molecular Simulation. 2019;45(9):685-693. https://doi.org/10.1080/08927022.2019.1579326

58. Bai Y, Ye F, Feng Y, et al. Structural basis for the inhibition of the SARS-CoV-2 main protease by the anti-HCV drug narlaprevir. Signal Transduction and Targeted Therapy. 2021;6(1):51. https://doi.org/10.1038/s41392-021-00468-9 PMid:33542181 PMCid:PMC7860160

59. Du L, He Y, Zhou Y, Liu S, Zheng BJ, Jiang S. The spike protein of SARS-CoV - a target for vaccine and therapeutic development. Nat Rev Microbiol. 2009;7(3):226-236. https://doi.org/10.1038/nrmicro2090 PMid:19198616 PMCid:PMC2750777

60. Moelyadi F, Utami PD, Dikman IM. Inhibitory Effect of Active Substances of Lollyfish (Holothuria atra) Against the Development of Plasmodium falciparum Based on In Silico Study. Indo J Mar Sci. 2020;25(4):135-142. https://doi.org/10.14710/ik.ijms.25.4.135-142

61. Sharma SK, Parasuraman P, Kumar G, Surolia N, Surolia A. Green Tea Catechins Potentiate Triclosan Binding to Enoyl-ACP Reductase from Plasmodium falciparum (PfENR). J Med Chem. 2007;50(4):765-775. https://doi.org/10.1021/jm061154d PMid:17263522

62. Tegar M, Purnomo H. Tea Leaves Extracted as Anti-Malaria based on Molecular Docking PLANTS. Procedia Environmental Sciences. 2013;17:188-194. https://doi.org/10.1016/j.proenv.2013.02.028

63. Pokharkar O, Lakshmanan H, Zyryanov G, Tsurkan M. In Silico Evaluation of Antifungal Compounds from Marine Sponges against COVID-19-Associated Mucormycosis. Marine Drugs. 2022;20(3):215. https://doi.org/10.3390/md20030215 PMid:35323514 PMCid:PMC8950821